

ORIGINAL  
ARTICLETransplanted microvascular endothelial cells  
promote oligodendrocyte precursor cell survival  
in ischemic demyelinating lesions

Keiya Iijima,\* Masashi Kurachi,† Koji Shibasaki,† Masae Naruse,†  
Sandra Puentes,\* Hideaki Imai,‡ Yuhei Yoshimoto,\* Masahiko Mikuni§ and  
Yasuki Ishizaki†

\*Department of Neurosurgery, Gunma University Graduate School of Medicine, Maebashi, Gunma,  
Japan

†Department of Molecular and Cellular Neurobiology, Gunma University Graduate School of Medicine,  
Maebashi, Gunma, Japan

‡Department of Neurosurgery, Tokyo University Graduate School of Medicine, Bunkyo-ku, Tokyo, Japan

§Department of Psychiatry and Neuroscience, Gunma University Graduate School of Medicine,  
Maebashi, Gunma, Japan

**Abstract**

We previously showed that transplantation of brain microvascular endothelial cells (MVECs) greatly stimulated remyelination in the white matter infarct of the internal capsule (IC) induced by endothelin-1 injection and improved the behavioral outcome. In the present study, we examined the effect of MVEC transplantation on the infarct volume using intermittent magnetic resonance image and on the behavior of oligodendrocyte lineage cells histochemically. Our results *in vivo* show that MVEC transplantation reduced the infarct volume in IC and apoptotic death of oligodendrocyte precursor cells (OPCs). These results indicate that MVECs have a survival effect on OPCs, and this effect might contribute to the recovery of the white matter infarct.

The conditioned-medium from cultured MVECs reduced apoptosis of cultured OPCs, while the conditioned medium from cultured fibroblasts did not show such effect. These results suggest a possibility that transplanted MVECs increased the number of OPCs through the release of humoral factors that prevent their apoptotic death. Identification of such humoral factors may lead to the new therapeutic strategy against ischemic demyelinating diseases.

**Keywords:** cell survival, cerebral microvascular endothelial cells, cerebral small vessel disease, oligodendrocyte, precursor cell, remyelination.

*J. Neurochem.* (2015) **135**, 539–550.

Ischemic demyelination is a result of either subcortical white matter stroke, which accounts for 15–25% of all stroke subtypes (Bamford *et al.* 1991), or of cerebral small vessel disease, which has become more common as the population ages, and has no specific treatment (Nitkunan *et al.* 2008; Conijn *et al.* 2011; Khalilzada *et al.* 2011; Wardlaw *et al.* 2013). We have been investigating the cell–cell interaction between brain microvascular endothelial cells (MVECs) and neural cells to develop therapeutics for ischemic demyelinating diseases. This cell–cell interaction is known as the neurovascular unit and is important in homeostasis and repair of the brain. Studies to analyze the cell–cell interaction between MVECs and neural cells have mainly been performed *in vitro*,

Received June 2, 2015; revised manuscript received July 20, 2015; accepted July 21, 2015.

Address correspondence and reprint requests to Yasuki Ishizaki, Department of Molecular and Cellular Neurobiology, Gunma University Graduate School of Medicine, 3-39-22 Showa-machi, Maebashi, Gunma 371-8511 Japan. E-mail: yasukiishizaki@gunma-u.ac.jp

**Abbreviations used:** BSA, bovine serum albumin; CM, conditioned medium; DMEM, Dulbecco's modified Eagle medium; ET-1, endothelin-1; FBS, fetal bovine serum; HBSS, Hank's balanced salt solution; IC, internal capsule; LFB, luxol fast blue; MR, magnetic resonance; MVEC, microvascular endothelial cell; OL, oligodendrocyte; OPC, oligodendrocyte precursor cell; PBS, phosphate-buffered saline; PDGF, platelet-derived growth factor; PDGFR, platelet-derived growth factor receptor; PDL, poly-D-lysine; PLP, proteolipid protein; SD, Sprague-Dawley; TNB, Tris-NaCl-blocking; TUNEL, terminal deoxynucleotidyl transferase-mediated dUTP nick-end labeling.

and *in vivo* studies could not exclude the effect of increased blood flow (Muramatsu *et al.* 2012; Ishikawa *et al.* 2013). Some studies reported that angiogenesis promotes neurogenesis or lesion volume reduction (Hayashi *et al.* 1998; Zhang *et al.* 2000; Louissaint *et al.* 2002; Sun *et al.* 2010; Uemura *et al.* 2012), whereas other studies revealed that revascularization of established brain ischemic lesions does not improve the outcome for patients (Hacke *et al.* 2008; Sandercock *et al.* 2012). Our previous study showed that the volume of ischemic demyelinating lesions decreased in the absence of increased vascularization after transplantation of MVECs (Puentes *et al.* 2012), suggesting that the direct cell–cell interaction between MVECs and neural cells is important in this therapeutic effect.

In the present study, MVECs prepared from rat cerebral cortex were transplanted into an endothelin-1 (ET-1)-induced demyelinating lesion (infarct), and changes in the infarct volume and in the behavior of oligodendrocyte (OL) lineage cells were investigated. Transplanted MVECs reduced the ischemic white matter infarct volume, increased the number of OL lineage cells without promoting their proliferation, and inhibited the apoptotic death of oligodendrocyte precursor cells (OPCs) in ischemic demyelinating lesions. The cell–cell interaction between MVECs and OL lineage cells is called the oligovascular niche, and may be important in the survival of OPCs (Arai and Lo 2009). These findings may be helpful for developing new therapeutic tools against ischemic demyelinating diseases. In this study, we used bovine serum albumin (BSA) as control, because we confirmed that transplantation of meningeal cells, another cell type, had no therapeutic effects on ischemic white matter damage in our previous study (Puentes *et al.* 2012).

## Materials and methods

### Animals

We used adult male Sprague-Dawley (SD) rats (weighing 200–250 g at the beginning of experiments; Harlan Sprague Dawley, Indianapolis, IN, USA). All procedures were performed in accordance with the guidelines for Animal Experimentation at Gunma University Graduate School of Medicine and were approved by Gunma University Ethics Committee. These procedures were also in accordance with EC Directive 86/609/EEC and the Uniform Requirements for Manuscripts Submitted to Biomedical Journals. All surgical procedures were conducted under aseptic conditions, and every effort was made to minimize animal suffering and to reduce the number of animals used.

### Magnetic resonance imaging

Magnetic resonance (MR) imaging was carried out on day 7 after ET-1 injection before MVEC transplantation or vehicle injection, and on day 21 by a 1-T benchtop MR scanner (Icon; Bruker Biospin GmbH, Ettlingen, Germany) (Schmid *et al.* 2013). Anesthesia was induced with 5% isoflurane and maintained with 1.5% isoflurane (in room air). Respiration rates were monitored throughout the

procedure, and body temperature was maintained at 37°C. A rapid acquisition relaxation enhancement, low resolution T2-weighted sequence was used to determine the precise lesion location: rapid-acquisition relaxation enhancement factor 5, repetition time 2500 ms, echo time 60 ms with in-plane resolution of  $266 \times 266 \mu\text{m}^2$ , thickness 1250  $\mu\text{m}$ , and 9 slices. A second high-resolution T2-weighted imaging set was acquired throughout the lesion: rapid-acquisition relaxation enhancement factor 10, repetition time 2500 ms, echo time 80 ms with in-plane resolution of  $143 \times 143 \mu\text{m}^2$ , thickness 1000  $\mu\text{m}$ , and 10 contiguous slices. The lesion and the internal capsule (IC) were manually delineated from the high-resolution MR images and the lesion volume in the IC was calculated. T2\*-weighted sequence was used to detect iron-labeled MVECs: Fast low angle shot, repetition time 800 ms, echo time 20 ms with in-plane resolution of  $266 \times 266 \mu\text{m}^2$ , thickness 1250  $\mu\text{m}$ , and 9 slices.

### Cell culture

MVECs were prepared from the cerebra of green rats [SD-Tg(CAG-EGFP)] (for transplantation) or wild-type rats (for preparation of conditioned medium, CM) according to Puentes *et al.* (2012) and Szabó *et al.* (1997). For iron labeling, we used Ferumoxides (Feridex; Eiken Chemical, Tokyo, Japan) according to Arbab *et al.* (2005) with some modifications. Protamine sulfate was added to MVEC culture medium (Puentes *et al.* 2012) containing 50 mg/mL Ferumoxides to the concentration of 5 mg/mL. After mixing by intermittent manual shaking for 3–5 min, we replaced the medium of MVEC culture by this mixture. The cells were then incubated overnight, and washed with sterile phosphate-buffered saline (PBS), and then with PBS-containing heparin (10 U/mL) to dissolve extracellular Ferumoxides–protamine complexes before harvesting for transplantation.

OPCs were prepared from the cerebra of SD rats (postnatal days 1–2). The cortical tissue was digested with 16.5 U/mL papain solution, triturated, and centrifuged. The pellet was suspended in the panning buffer (5  $\mu\text{g}/\text{mL}$  insulin, 0.02% BSA in Hank's balanced salt solution, HBSS). Dissociated cells were immunopanned on anti-RAN-2, anti-galactocerebroside, and O4 antibody-coated plates. OPCs isolated as O4-positive cells were suspended in Dulbecco's modified Eagle medium (DMEM)-F12 containing 100 U/mL penicillin, 100  $\mu\text{g}/\text{mL}$  streptomycin, 1 mM sodium pyruvate, 5  $\mu\text{g}/\text{mL}$  insulin, 100  $\mu\text{g}/\text{mL}$  apotransferrin, 100  $\mu\text{g}/\text{mL}$  BSA, 62 ng/mL progesterone, 16  $\mu\text{g}/\text{mL}$  putrescine, 40 ng/mL sodium selenite, and 30  $\mu\text{M}$  *N*-acetyl cysteine (DMEM-F12/SATO). The cells were plated into poly-D-lysine-coated tissue culture dish, and grown in DMEM-F12/SATO medium containing forskolin, ciliary neurotrophic factor, neurotrophin-3, and platelet-derived growth factor (PDGF)-AA. After several days, OPCs were harvested from the dish, using TrypLE Express (Invitrogen, Carlsbad, CA, USA), washed, and suspended in the culture medium. OPCs were plated on poly-D-lysine-coated 8-well glass slides at the density of 12 000 cells/cm<sup>2</sup>.

Rat fibroblast-like cells (Rat-1) were cultured in DMEM containing 10% fetal bovine serum on collagen type I-coated dish.

### Stereotactic ET-1 injection and cell transplantation

ET-1 injection was performed as previously described with some modifications (Puentes *et al.* 2012). SD rats (8-week-old) were anesthetized and placed in a stereotactic frame. The posterior limb

of the IC was targeted for injection (2.3 mm posterior and 6.1 mm lateral left to the bregma, 3.7 mm depth, angle 25°). One microliter of ET-1 solution (200 pmol/μL, peptide) was injected at a constant flow rate (0.5 μL/min). Seven days after ET-1 injection, when the ischemic injury had been established, 2 μL of the cell suspensions (MVECs suspended in 0.2% BSA–HBSS) at the density of  $4 \times 10^4$  cells/μL or 0.2% BSA–HBSS was injected into each animal using the coordinates used for ET-1 injection.

### Cryosection

Cryosection was performed as previously described with some modifications (Puentes *et al.* 2012). The animals were anesthetized with isoflurane and perfused transcardially with saline solution containing 10 U/mL heparin, followed by 0.1 M phosphate buffer (pH 7.4) containing 4% paraformaldehyde. The brain was immediately dissected, postfixed 60 min in the same fixative at 4°C, cryoprotected with 30% sucrose in 0.1 M phosphate buffer, and finally frozen with optimal cutting temperature compound. Frozen coronal sections (20 μm in thickness, 120 serial slices per brain) were cut on a cryostat (CM3050S; Leica Biosystems, Nussloch, Germany), mounted on pre-coated glass slides (Matsunami, Osaka, Japan), and placed at 23°C for 1 h to air dry. The sections were stored at –80°C until staining.

### Immunostaining for NG2, MBP, CC1, ED-1, PDGFRα and neurofilament proteins

Primary antibodies for immunostaining included mouse monoclonal antibodies directed against CC1 (1 : 400; EMD Millipore, Billerica, MA, USA), SMI31 (recognizing phosphorylated neurofilament (NF) heavy chain, 1 : 1000; BioLegend, San Diego, CA, USA), ED-1 (1 : 100; AbD Serotec, Kidlington, Oxfordshire, UK) and SMI94 [recognizing myelin basic protein (MBP), 1 : 400; BioLegend]; and rabbit polyclonal antibodies directed against NG2 and platelet-derived growth factor receptor (PDGFR)α (1 : 200; EMD Millipore). Sections were air-dried at 23°C, fixed with 4% paraformaldehyde, incubated with 2% BSA in PBS containing 10% normal donkey serum and 0.3% Triton X-100 (or without detergent for NG2 antigen) for 30 min, and then incubated with primary antibodies overnight at 4°C overnight. After washing with PBS, sections were incubated with fluorophore-conjugated secondary antibodies: rhodamine-conjugated donkey anti-mouse IgG (Jackson ImmunoResearch, West Grove, PA, USA) for SMI94; rhodamine-conjugated goat anti-rabbit Ig (Jackson ImmunoResearch) for NG2, when co-stained with terminal deoxynucleotidyl transferase-mediated dUTP nick-end labeling (TUNEL); Alexa Fluor 488-conjugated goat anti-rabbit Ig (Invitrogen) for NG2, when co-stained for MBP; Alexa Fluor 488-conjugated donkey anti-rabbit Ig (Invitrogen) for PDGFRα; and Alexa Fluor 488-conjugated donkey anti-mouse Ig (Invitrogen) for CC1 and SMI31. We used a tertiary antibody, Alexa Fluor 568-conjugated donkey anti-goat Ig (Invitrogen), when NG2 was co-stained with TUNEL. Hoechst 33342 (Sigma-Aldrich, St Louis, MO, USA) was used for nuclear staining. Sections were examined using a fluorescence microscope (Keyence, Osaka, Japan).

### Immunostaining for Ki67 and Olig2

The brain sections were air-dried at 23°C, washed with PBS followed by distilled water, then fixed with 4% paraformaldehyde

for 10 min. Antigen retrieval was performed at 120°C for 20 min in trisodium citrate buffer (10 mM, pH 6.0). The sections were then incubated in 3% H<sub>2</sub>O<sub>2</sub> in PBS for 10 min, and followed in Tris–NaCl-blocking (TNB) buffer (0.1 M Tris–HCl, 0.15 M NaCl) containing 0.5% Blocking reagent (PerkinElmer, Waltham, MA, USA) before incubation with mouse monoclonal anti-Ki67 antibody (1 : 400; BD-Pharmingen, San Jose, CA, USA) and rabbit polyclonal anti-Olig2 antibody (1 : 200; IBL, Takasaki, Japan) diluted in TNB buffer overnight at 4°C. After washing with PBS, the sections were incubated with biotin-conjugated anti-mouse antibody (1 : 1500; Jackson ImmunoResearch) and rhodamine-conjugated goat anti-rabbit antibody (1 : 100) for 120 min, washed again in PBS, and then incubated with Streptavidin-horseradish peroxidase (1 : 1500; PerkinElmer) and Alexa Fluor 568-conjugated donkey anti-goat antibody (1 : 500) for 120 min. The Ki67 signal was enhanced, using Tyramide Signal Amplification methods (TSA Plus Fluorescein Evaluation Kit; PerkinElmer). Hoechst 33342 was used for nuclear staining.

### Double labeling for TUNEL and NG2

TUNEL staining was performed using the TACS2 TdT-Fluor *In Situ* Apoptosis Detection Kit (Trevigen, Gaithersburg, MD, USA) according to the manufacturer's instructions. After washing sections in distilled water, Streptavidin-horseradish peroxidase (diluted 1 : 300 in PBS) was applied to each section for 1 h at 23°C. The positive reaction was detected using Tyramide Signal Amplification methods. After TUNEL staining, the sections were fixed in 4% paraformaldehyde for 10 min, incubated with 2% BSA-PBS containing 10% donkey serum for 30 min, and then incubated in anti-NG2 antibody (1 : 200) overnight at 4°C. After washing with PBS, sections were incubated with rhodamine-conjugated goat anti-rabbit antibody for 120 min, and then incubated with Alexa Fluor 568-conjugated donkey anti-goat antibody. Hoechst 33342 was used for nuclear staining.

### In situ hybridization

*In situ* hybridization was performed as previously described (Shibasaki *et al.* 2007). Briefly, digoxigenin-labeled antisense/sense probes were used for *in situ* hybridization of proteolipid protein (PLP). The 1.4 kb fragment of mouse PLP1 cDNA was subcloned into pSPT18 by BamHI and EcoRI sites (Dr. K. Ikenaka kindly provided us this vector (Ivanova *et al.* 2003)). The cDNA fragment has high homology against rat PLP1. After we linearized the plasmid (antisense: BamHI, sense: EcoRI), the digoxigenin-labeled antisense/sense probes were synthesized by RNA polymerase (antisense: T7 RNA polymerase, sense: SP6 RNA polymerase). Detection of mRNA on cryo-sectioned tissues was performed by nitroblue tetrazolium/5-bromo-4-chloro-3-indolyl phosphate through an alkaline phosphatase-conjugated anti-digoxigenin antibody (Roche, Basel, Switzerland).

### Conditioned media and OPC survival assay

To prepare conditioned media, we used MVECs (90–95% confluence) and Rat-1 cells (60–70% confluence) grown in DMEM-F12/SATO medium for 48 h. Conditioned media were collected, and centrifuged to remove cell debris. The supernatant was filtered with a 0.45 μm filter and used without dilution. OPCs plated on 8-well glass slides were washed with PBS, and then cultured in conditioned

media from MVECs (MVEC-CM) or Rat-1 cells (Rat-1-CM). As control, OPCs were cultured in DMEM-F12/SATO medium. After 2 days, OPCs were vitally stained with Hoechst 33342. All cells (both pyknotic and non-pyknotic) were counted and the fraction of pyknotic cells was determined.

### Statistical analysis

Data are presented as the mean  $\pm$  SE of the mean. For analysis of lesion volume on MR imaging and pyknotic nuclear ratio of OPCs, differences between groups were analyzed with one-way analyses of variance followed by the *post hoc* Tukey–Kramer test. For analyses of cell density of OPCs, OL lineage cells as well as immature and mature OLs, TUNEL positive ratio of OPCs, and proliferation ratio of OL lineage cells, differences between groups were examined by Student's *t*-test. Cell counting was performed by researchers unaware of the profile of the animals.

## Results

### Change in the infarct volume revealed by MR imaging

Although we reported that MVEC transplantation ameliorated ischemic damage in IC, we did not follow the change in the infarct volume in IC of the same animals, as we evaluated ischemic damage histochemically and had to sacrifice animals at each time point (Puentes *et al.* 2012). To confirm the therapeutic effect of MVEC transplantation in the same animals, we used MR imaging. At first we examined whether our MVEC transplantation into IC was successful or not by MR imaging (Fig. 1a). To visualize MVECs, we labeled cultured MVECs with iron before transplanting them into IC. The MR imaging revealed the presence of MVECs 7 days after transplantation, showing that our transplantation was successful. MVECs appeared to remain in the transplanted site as a lump, confirming our previous observation that only a few of the transplanted MVECs were incorporated into host vasculatures (see Fig. 6

in Puentes *et al.* 2012). We then quantified the infarct volume in IC using MR imaging. The size of the histological demyelinating lesion revealed by luxol fast blue (LFB) staining correlated with the infarct size calculated by T2-weighted MR Imaging (Fig. 1b and c) as previously reported (Lecrux *et al.* 2008). Representative MR images of each group in our experimental schedules (Fig. 2a) are shown in Fig. 2b. In Fig. 2, ‘No treatment’

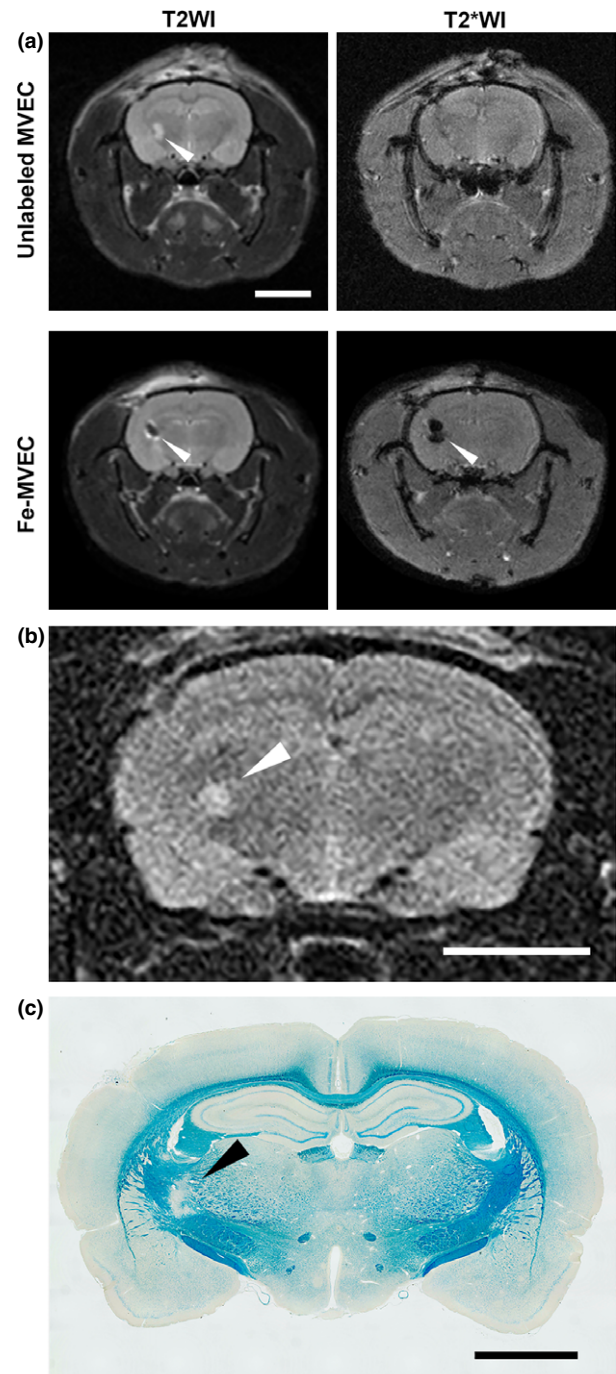
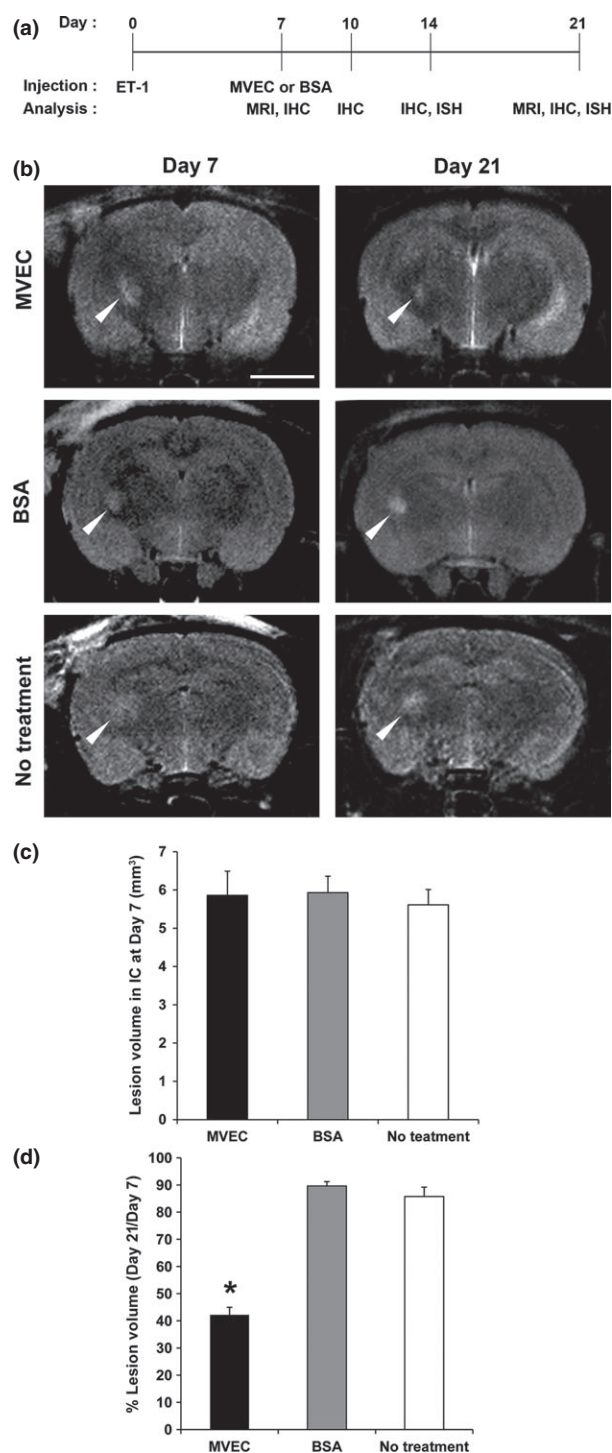


**Fig. 1** Magnetic resonance (MR) imaging of iron-labeled microvascular endothelial cells (MVECs) and correlation between MR image and luxol fast blue (LFB)-stained section of endothelin-1 (ET-1)-induced ischemic demyelinating lesion. (a) T2-weighted (left column) and T2\*-weighted (right column) MR images of rat brain with white matter infarct in the internal capsule induced by ET-1 injection. Unlabeled MVECs (upper row) or iron-labeled MVECs (lower row) were stereotactically transplanted into the infarct 7 days after ET-1 injection. The images were obtained 7 days after MVEC transplantation. Arrowheads show the location of infarct and transplanted cells. Iron-labeled MVECs can be detected as low intensity area. The low intensity area of iron-labeled MVECs can be enhanced using T2\*-weighted image. Scale bar = 10 mm. (b) T2-weighted MR image of rat brain 11 days after ET-1 injection. Arrowhead shows the infarct on T2-weighted MR image. Scale bar = 5 mm. (c) LFB-stained section of the same animal as shown in (b) that was killed just after MR imaging. Arrowhead shows the infarct on LFB-stained section. Scale bar = 2.5 mm.



means animals receiving ET-1 injection on day 0 and no treatment thereafter. At day 7, no significant difference was found in the volume of the infarct in IC between each group (Fig. 2c). The percentage of the infarct volume in IC at day 21 relative to that of day 7 was significantly smaller in the MVEC-transplanted group compared to control

**Fig. 2** Experimental designs and analyses of the change in the lesion volume in the internal capsule (IC) measured by magnetic resonance (MR) imaging. (a) Experimental designs. Endothelin-1 (ET-1) was injected into the left IC stereotactically to induce ischemic demyelination at day 0. Microvascular endothelial cell (MVECs) or bovine serum albumin (BSA) were injected into each animal using the initial coordinates at day 7. Samples for immunohistochemical analysis were obtained from animals at days 7, 10, 14, and 21. MR imaging was performed at days 7 and 21. (b) MR images obtained at days 7 and 21. 'No treatment' means animals receiving ET-1 injection on day 0 and no treatment thereafter. Scale bar: 5 mm. (c) Quantification of the lesion volume in IC at day 7. There was no significant difference between animals treated differently afterwards ( $n = 5$ ). (d) Quantification of the percentage lesion volume in the IC at day 21 relative to that at day 7. This volume was significantly smaller in MVEC-transplanted animals compared to animals treated with BSA or untreated ( $n = 5$ , each). \* $p < 0.05$ .

groups treated with BSA, or untreated (Fig. 2d). Remyelination was observed in the region where transplanted MVEC had no direct contact with the lesion (data not shown), confirming our previous results (see Fig. 5b in Puentes *et al.* 2012). This suggests that the transplanted MVEC might release some humoral factors to induce remyelination. In our previous histochemical study, we examined the infarct volume at only one time point in each animal (Puentes *et al.* 2012). Using MR imaging, however, we succeeded in confirming that MVEC transplantation reduces the infarct volume in the same animal by day 21.

#### Axons were preserved in ET-1-induced demyelinating lesion

To evaluate whether the axons indispensable for remyelination were preserved in ET-1-induced lesion in the IC, we examined the axons in ET-1-treated IC using immunostaining for neurofilament proteins. Demyelinating lesions were identified with a bright field microscope (Figure S1, left column). In Figure S1, 'Intact IC' means the IC that received no intervention at all. Immunohistochemical staining for neurofilament proteins revealed the profiles of the axons (Figure S1, right column). Presence of axons was confirmed in the lesion in IC at day 7 (data not shown), and in the lesions of animals treated with MVECs or BSA at day 14 (Figure S1b and c). There was no apparent difference in the density of axons in IC between three groups (intact, MVEC-treated, or BSA-treated) at day 14 (Figure S1). These results suggest that axons were preserved in the ET-1-induced demyelinating lesions.

#### MVECs increased OPCs in the lesion

To elucidate the cellular mechanism whereby MVEC transplantation promotes remyelination in the lesion, we focused on OPCs, because they play an important role in remyelinating process in other demyelinating diseases like

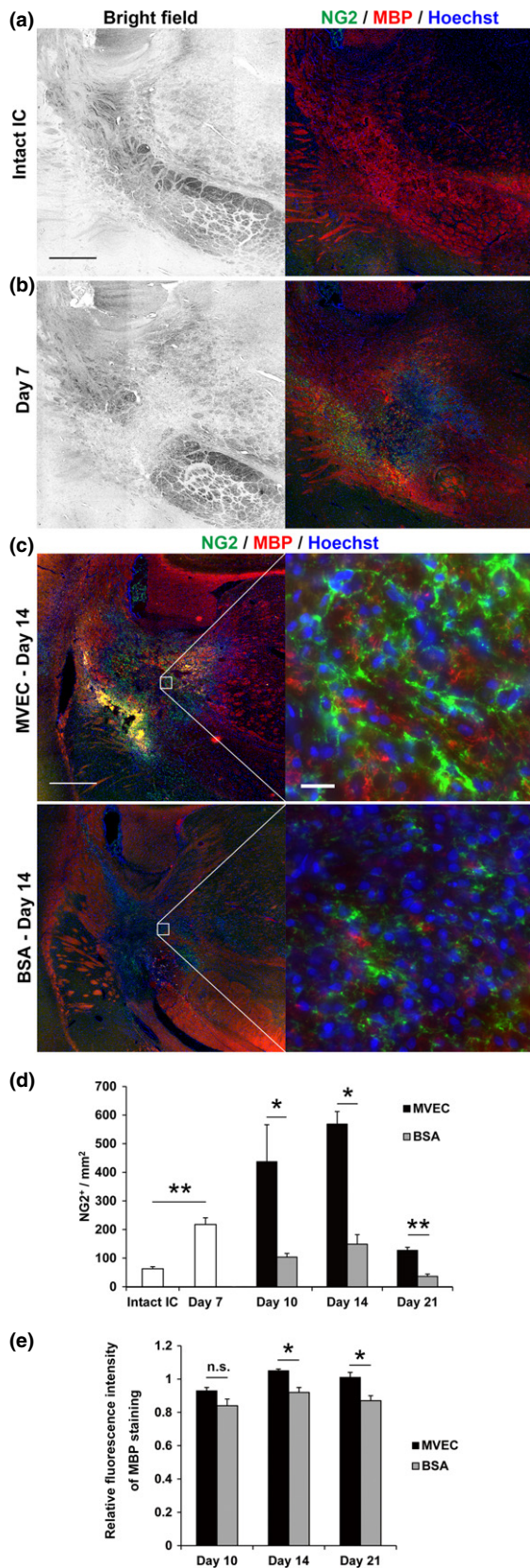


**Fig. 3** Microvascular endothelial cell (MVEC) transplantation increased the number of oligodendrocyte precursor cells (OPCs) and fluorescence intensity of myelin basic protein (MBP) staining. ‘Intact internal capsule (IC)’ means the IC that received no intervention at all. Sections were double immunostained for NG2 and MBP, a marker for myelin. Nuclei were stained with Hoechst 33342. Bright field (left) and double immunostaining (right) images of the normal IC (a) and the lesion in the endothelin-1 (ET-1)-injected IC at day 7 (b). Scale bar: 500  $\mu$ m. The signal for MBP was reduced in the ET-1-injected IC, whereas the signal for NG2 increased in the injured IC. (c) Double immunostaining for NG2 and MBP of the ET-1-injected IC treated with MVECs (upper row) or bovine serum albumin (BSA) (lower row) at day 14. Images in the left column show the location of lesions in the IC. Higher magnification images of the insets in the left column are shown in the right column. Scale bar in the left column: 500  $\mu$ m, and scale bar in the right column: 20  $\mu$ m. Note that signals for both NG2 and MBP increased in the MVEC-treated IC. (d) Quantification of densities of NG2-positive cells (OPCs) in the normal IC, in the lesion in the IC at day 7, and in the lesions in the ET-1-injected IC treated with MVECs or BSA (on day 7) analyzed at days 10, 14, and 21. \* $p < 0.05$ , \*\* $p < 0.01$  ( $n = 3-5$ ). (e) Quantification of relative fluorescence intensity of MBP staining in the ET-1-injected IC at days 10, 14, and 21. The fluorescence intensities of the whole IC regions on ET-1-injected side and those on the contralateral side were measured, and the ratios of the intensities on ET-1-injected side to those on the contralateral side were shown. As control, BSA-injected animals were used. \* $p < 0.05$  ( $n = 3-5$ ).

multiple sclerosis (Miron *et al.* 2011). We initially assessed the distribution of OPCs in and around the lesion in IC. Brain sections were immunostained with antibodies against NG2, a marker for OPCs, and MBP, a marker for myelin (Fig. 3). In Fig. 3, ‘Intact IC’ means the IC that received no intervention at all. Immunohistochemical staining for NG2 revealed the presence of OPCs in the brain. NG2 expression *in vivo* has also been detected in microglia/macrophages (Jones *et al.* 2002) and pericytes (Dore-Duffy *et al.* 2006). We confirmed, however, that NG2-positive cells did not co-express ED-1, a marker for microglia/macrophages, in our experiments (Figure S2). We observed that pericytes also express NG2 in our experiments. They were, however, easily distinguished from OPCs, as they were always localized within vasculatures and displayed different morphology. In ET-1-injected IC, MBP signal was remarkably reduced, confirming demyelination in the lesion (Fig. 3c). To ask whether the cell density of OPCs in the lesion changed with time after ET-1 injection and MVEC transplantation, we counted the number of OPCs (NG2-positive cells) and estimated their cell densities in the normal IC, in the lesions in IC of ET-1-treated animals at day 7, and in the lesions in IC of ET-1-injected animals that received MVECs or BSA (on day 7) at days 10, 14, and 21. The density of OPCs significantly increased in the lesion in IC at day 7 compared

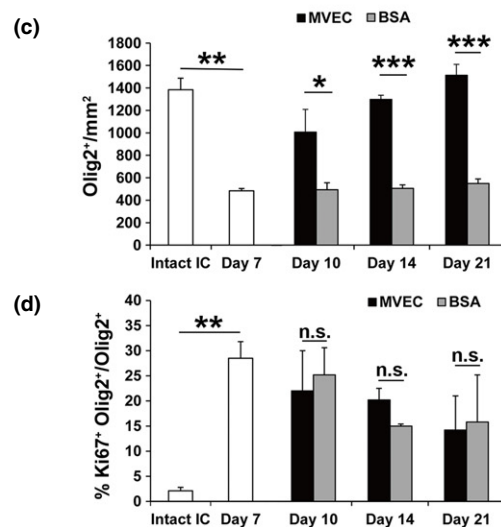
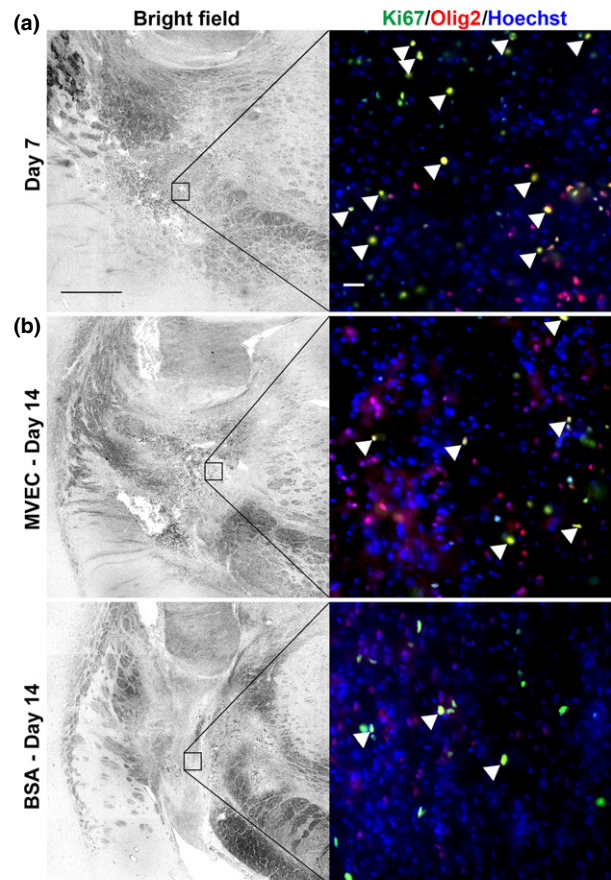
to the normal IC (Fig. 3a, b, and d). The density of OPCs in the lesion in IC of MVEC-transplanted animals gradually increased up to day 14 and then decreased down to day 21, whereas the density in the lesion in IC of BSA-treated animals decreased in comparison to day 7. The densities of OPCs in the lesion in the IC were significantly higher in MVEC-treated animals compared to BSA-treated animals at days 10, 14, and 21 (Fig. 3c and d). At days 14 and 21, MBP staining showed higher remyelination in the MVEC-treated IC compared to the BSA-treated IC (Fig. 3c and e). These results indicate that MVEC transplantation induced not only enhanced myelination as previously reported (Puentes *et al.* 2012), but also exhibited an increase in the density of OPCs in the lesion.

#### MVECs did not stimulate OPC proliferation

To ask whether an increase in the density of OPCs in the lesion in MVEC-treated animals was caused by their proliferation, we analyzed proliferative OL lineage cells using antibodies against Olig2, a marker for OL lineage cells, and Ki67, a marker for proliferative cells. Olig2/Ki67 double positive cells can be regarded as OPCs, because OLs, both immature and mature, have exited the cell cycle and thus non-proliferative (Nishiyama *et al.* 2009). Immunohistochemical staining for Olig2 revealed that the density of OL lineage cells was significantly lower in the lesion in the IC at day 7 compared to the intact IC (Fig. 4c). Cell densities of OL lineage cells were significantly higher in MVEC-treated animals compared to BSA-treated animals at days 10, 14, and 21 (Fig. 4c). Moreover, OL lineage cells increased gradually from days 10 to 21 in MVEC-treated animals (Fig. 4c).

**Fig. 4** Microvascular endothelial cell (MVEC) transplantation did not enhance proliferation of oligodendrocyte (OL) lineage cells. Sections were double stained for Ki67 and Olig2. Nuclei were stained with Hoechst 33342. Representative images of the lesion in the endothelin-1 (ET-1)-injected IC analyzed at day 7 (a), and the lesion in the ET-1-injected IC treated with MVECs (upper row) or bovine serum albumin (BSA) (lower row) (on day 7) analyzed at day 14 (b). Bright field images are shown in the left column, and higher magnification images of the insets in the left column are shown in the right column. White arrowheads indicate cells positive for both Ki67 and Olig2 (proliferating oligodendrocyte precursor cells, OPCs). Scale bar in the left column: 500  $\mu$ m, and scale bar in the right column: 20  $\mu$ m. (c) Densities of Olig2-positive cells (OL lineage cells) in the normal IC, in the lesion in the ET-1-injected IC analyzed at day 7, and in the lesions in the ET-1-injected IC treated with MVECs or BSA (on day 7) analyzed at days 10, 14, and 21.  $*p < 0.05$ ,  $**p < 0.01$ ,  $***p < 0.001$  ( $n = 3-5$ ). (d) Percentage of cells positive for both Ki67 and Olig2 (proliferating OPCs) relative to Olig2-positive cells (OL lineage cells) in the normal IC, in the lesion in the ET-1-injected IC analyzed at day 7, and in the lesion in the ET-1-injected IC treated with MVECs or BSA (on day 7) analyzed at days 10, 14, and 21.  $**p < 0.01$ , n.s.: not significant ( $n = 3-5$ ).

Double immunostaining for Olig2 and Ki67 revealed that proliferation of OL lineage cells in the lesion in IC was not significantly higher in MVEC-treated animals compared to BSA-treated animals at days 10, 14, and 21 (Fig. 4b and d). These results suggest that MVEC transplantation does not stimulate proliferation of OPCs in the lesion.



### MVECs promoted OPC survival

We examined survival of OPCs using TUNEL assay combined with NG2 immunostaining. At day 7, about 16% of OPCs in the demyelinating lesions were apoptotic (Fig. 5a and d). Representative images of TUNEL and NG2 staining at day 10 are shown in Fig. 5(b) and (c). The percentage of TUNEL-positive (apoptotic) OPCs (NG2-positive cells) in the lesion in IC was significantly smaller in MVEC-treated animals than that in BSA-treated animals at days 10 and 14 (Fig. 5d). These results indicate that MVEC transplantation promoted OPC survival in the infarct in IC.

### MVECs increased immature OLs but not mature OLs

We then examined whether MVEC transplantation increased mature OLs in the lesion in IC by *in situ* hybridization for *PLP* mRNA, a marker for mature OLs, and immunostaining for CC1 – a marker for both immature and mature OLs – as increased myelination might be because of an increase in mature OLs. Contrary to our expectation, *in situ* hybridization for *PLP* mRNA revealed that there was no difference in the density of PLP-positive mature OLs between MVEC- and BSA-treated animals at days 14 and 21 (Figure S3a and c). By contrast, immunostaining for CC1 revealed that the density of CC1-positive cells was significantly higher in MVEC-treated animals compared to BSA-treated animals at day 14 (Figure S3b and d). These results suggest that enhanced myelination at day 21 is not the result of the increase in myelinating OLs.

### MVECs promoted survival of OPCs *in vitro*

To help clarify the mechanism by which MVECs promote survival of OPCs, we examined the effect of CM from MVEC cultures on OPC survival *in vitro*. OPCs were cultured with conditioned media from MVEC culture (MVEC-CM) or from Rat-1 culture (Rat-1-CM), or with the basal medium. After 2 days, cell death was assessed by staining nuclei with Hoechst 33342. In the presence of MVEC-CM, pyknotic OPCs were significantly fewer than those in the presence of Rat-1-CM or the basal medium (control), suggesting a possibility that humoral factors secreted from MVECs promote survival of OPCs in our ET-1-induced demyelinating lesion (Fig. 6a and b). As shown in Fig. 6(c), MVEC-CM *per se* apparently did not promote maturation of OPCs, judging from their morphology and PDGFR $\alpha$  expression, as OPCs cease PDGFR $\alpha$  expression once they differentiate into OLs (Nishiyama *et al.* 2009).

## Discussion

Our previous and present studies were graphically summarized in Fig. 7. In the present study, we confirmed the beneficial effect of MVEC transplantation on ET-1-induced

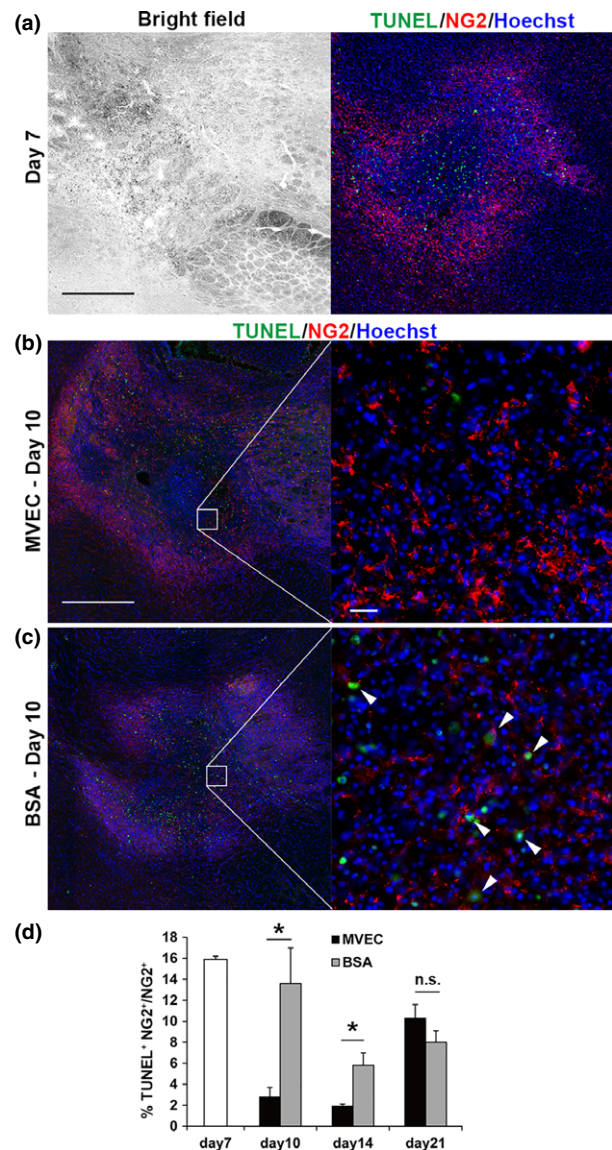


**Fig. 5** Microvascular endothelial cell (MVEC) transplantation reduced apoptotic cell death of oligodendrocyte precursor cells (OPCs). Sections were stained for NG2 and by terminal deoxynucleotidyl transferase-mediated dUTP nick-end labeling (TUNEL) to detect the apoptotic death of OPCs. Nuclei were stained with Hoechst 33342. Bright field (left) and double staining (right) images of the endothelin-1 (ET-1)-injected internal capsule (IC) at day 7 (a). Scale bar: 500  $\mu$ m. Double immunostaining images of lesions in the ET-1-injected IC treated with MVECs (b) or bovine serum albumin (BSA) (c) (on day 7) analyzed at day 10. Higher magnification images of insets in the left column are shown in the right column. Arrowheads indicate cells doubly positive for NG2 and TUNEL (apoptotic OPCs). Scale bar in the left column: 500  $\mu$ m, and scale bar in the right column: 30  $\mu$ m. (d) Quantification of TUNEL-positive (apoptotic) cells in NG2-positive cells (OPCs), in the ET-1-injected IC analyzed at day 7, and in the ET-1-injected IC treated with MVECs or BSA (on day 7) analyzed at days 10 and 14. \* $p < 0.05$  ( $n = 3-4$ ).



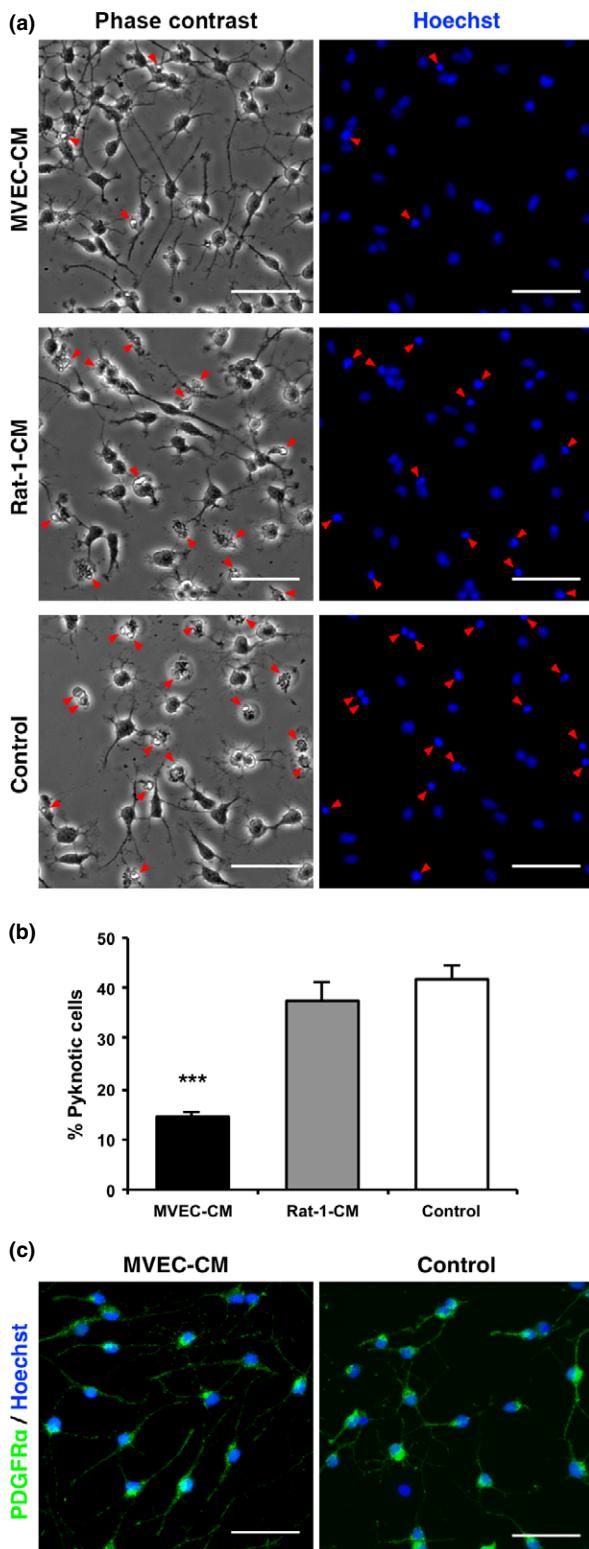


**Fig. 6** Conditioned medium (CM) from microvascular endothelial cell (MVEC) cultures reduced apoptosis of oligodendrocyte precursor cells (OPCs) but did not promote their maturation *in vitro*. OPCs prepared from neonatal rat brains were cultured with conditioned media from MVEC cultures (MVEC-CM), Rat-1 fibroblast cultures (Rat-1-CM), or with the basal medium (control) for 3 days. (a) Representative images of bright field (left) or Hoechst 33342 vital staining (right). Arrowheads indicate pyknotic cells. (b) Percentage of pyknotic cells. \*\*\* $p < 0.001$  ( $n = 2-3$ ). Note that the number of pyknotic cells was significantly reduced in the presence of MVEC-CM. (c) Representative images of anti-platelet-derived growth factor receptor (PDGFR) $\alpha$  staining of OPCs cultured with MVEC-CM or with the basal medium (control). Hoechst 33342 was used as a counter-stain. Apparent fewness of pyknotic cells in (c) was because of the loss of dead cells during washing procedures in immunostaining. Note that the morphology of OPCs and their PDGFR $\alpha$  expression were not affected by MVEC-CM treatment. Scale bars: 50  $\mu\text{m}$ .

2012), therapeutic effects were examined histologically, so that the change in the infarct volume could not be followed in the same animal but only be estimated from the data gathered from different animals. Our experimental system using MR imaging will prove useful for following the time course of white matter damage in rats or mice.

Gadea *et al.* (2009) reported that ET-1 produced and released by astrocytes regulates OL development via ET receptors expressed by OPCs. So there is a possibility that injected ET-1 directly affects OL lineage cells. Further studies are needed to examine this possibility.

The present study indicated that transplantation of MVECs induces an increase in the number of OPCs in ischemic demyelinating lesions, and that this increase in OPCs is mainly caused by inhibition of apoptotic death (Fig. 7c). Our previous study showed no change in the vascular densities in IC of MVEC-transplanted animals (Fig. 7a). These findings suggest that MVEC transplantation promotes survival of OPCs through the cell-cell interaction in the ischemic demyelinating lesion, independent of increased angiogenesis or higher blood flow. Previous studies of the treatment of ischemic brain lesion by increasing angiogenesis or blood flow could not distinguish the effect of the direct cell-cell interaction between MVECs and neural cells from the effect of increased blood flow (Hayashi *et al.* 1998; Zhang *et al.* 2000; Louissaint *et al.* 2002; Shin *et al.* 2008; Sun *et al.* 2010; Uemura *et al.* 2012). The present study clearly demonstrated that presence of MVECs *per se* has a beneficial effect on ischemic white matter damage *in vivo*, independent of increased angiogenesis. Our study also raises the possibility that malfunction of endothelial cells induces degeneration of OL lineage cells and results in demyelination. The findings of the present study are consistent with the previous report that OPCs are decreased through the apoptotic pathway in demyelinating lesions despite maintenance of the high proliferative rate (Payne *et al.* 2013) and suggest

ischemic damage to the white matter (Puentes *et al.* 2012), following the change in the infarct volume in the same animal using MR imaging (Fig. 7a and b). In many stroke studies thus far, including our previous one (Puentes *et al.*

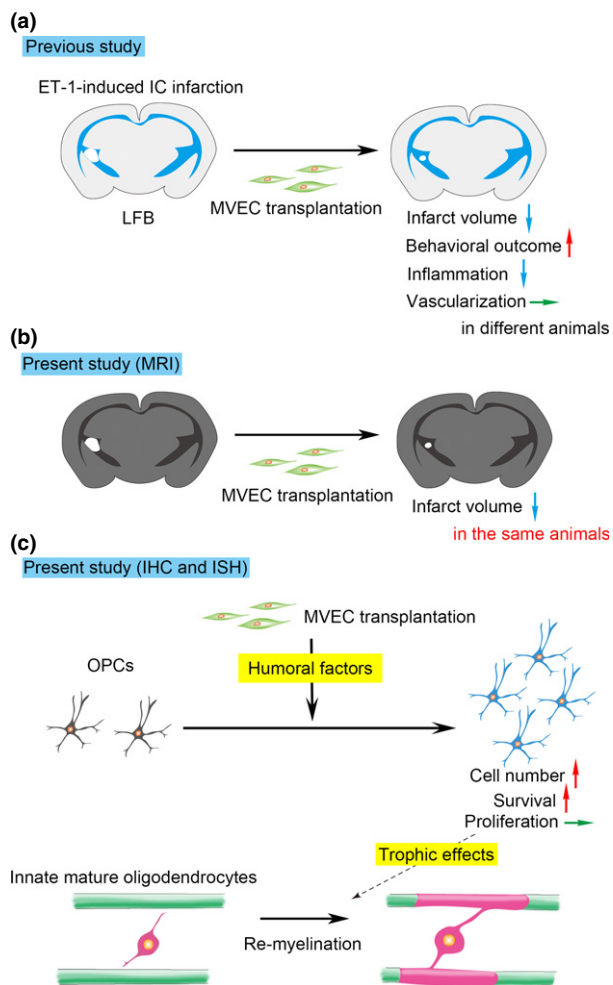


**Fig. 7** Graphical summary of our previous and present studies. (a) Our previous study. Microvascular endothelial cell (MVEC) transplantation reduced the volume of endothelin-1 (ET-1)-induced internal capsule (IC) infarction, improved the behavioral outcome, and repressed inflammation, although it did not promote vascularization. (b) Our present study (MRI). Therapeutic effects of MVEC transplantation were confirmed in the same animal. (c) Our present study (immunohistochemistry and *in situ* hybridization). MVEC transplantation increased oligodendrocyte precursor cells (OPCs) and immature oligodendrocytes (OLs) through promotion of OPC survival (not by enhancing OPC proliferation), although it did not increase mature OLs, suggesting increased OPCs and immature OLs improve myelination by existing (intrinsic) mature OLs through trophic effects.

that inhibition of the apoptotic death of OPCs is important for effective therapy of demyelinating diseases. At present, the molecular mechanism by which MVECs promote OPC survival remains undetermined. To help clarify this mechanism, we examined the effect of CM from MVEC culture on OPC survival *in vitro*, as the involvement of humoral factors was suggested in our *in vivo* studies. CM from MVEC culture significantly reduced apoptotic death of OPCs (Fig. 6), suggesting humoral factors released by MVECs

directly contribute to a decrease in the apoptotic death of OPCs. Previous studies have shown that cytokines released by infiltrating microglia/macrophages and/or reactive astrocytes induce apoptotic death of OPCs in demyelinating lesions (Rhodes *et al.* 2006; Schonberg *et al.* 2007; Fitzgerald *et al.* 2010). Our previous study also revealed that MVEC transplantation repressed the inflammatory response in the lesion (Fig. 7a), so there is a possibility that MVECs reduce apoptotic death of OPCs indirectly by inhibition of the inflammatory response.

From our *in vitro* study, MVEC-CM did not apparently promote maturation of OPCs (Fig. 6c). This did not coincide with our *in vivo* result, which revealed an increase in immature OLs by MVEC transplantation (Figure S3b and d). The reason for this discrepancy remains unclear at present. There is a possibility, however, that the humoral factors responsible for OPC maturation are not recovered at sufficient concentrations in CM in our experiments.

There is a possibility that an increase in OPCs results in an increase in myelinating mature OLs, thereby enhancing remyelination in the lesion. This seems unlikely, however, because MVEC transplantation increased OPCs and immature OLs but not mature OLs. From our previous and present studies, MVEC transplantation increased myelination, judging from LFB staining and MBP staining (Fig. 5 in Puentes *et al.* 2012; and Fig. 3 in this study). MVEC transplantation, however, did not increase the number of mature OLs (PLP-positive cells) at days 14 and 21 (Figure S3a and c), while it increased the number of immature OLs (CC1-positive cells) at day 14 (Figure S3b and d). This suggests that MVEC transplantation promotes myelination by existing (intrinsic) mature OLs without increasing their number (by the end of our observation period, day 21). At present, it remains unclear how MVEC transplantation and the resultant increase in OPCs and immature OLs promote remyelination in the lesion. Recently Porambo *et al.* (2015) reported that transplanted glial restricted precursor cells improve myelination through trophic effects in addition to differentiation into mature OLs. This suggests a possibility that increased OPCs and immature OLs improve myelination by existing mature OLs through trophic effects. Further studies are needed to address this point.

We have been examining the effects of vascular endothelial cells on OL lineage cells and revealed that vascular endothelial cells exert beneficial effects on OL lineage cells under pathological conditions. Recently Yuen *et al.* (2014) reported that OPCs induce angiogenesis via hypoxia-inducible factor (HIF) signaling during development. Taken together, there is a possibility that the interactions between vascular endothelial cells and OL lineage cells play important roles during development and recovery process under pathological conditions.

It may not be feasible to apply MVEC transplantation to the treatment of patients suffering from cerebral infarction.

Our study suggested, however, humoral factors released from MVECs promote OPC survival and increase their number, thereby enhancing remyelination in the lesion. Identification of such humoral factors and better understanding of the molecular mechanisms by which MVECs inhibit the apoptotic death of OPCs may lead to the establishment of a therapeutic strategy against ischemic demyelinating diseases.

## Acknowledgments and conflict of interest disclosure

We thank Dr. H. Ono (Department of Neurosurgery, Tokyo University Graduate School of Medicine) for advice on surgical techniques, and Dr. N. Yamane (Department of Neurosurgery, Gunma University Graduate School of Medicine), Ms. Y. Arai (Department of Pharmacy, Takasaki University of Health and Welfare, Takasaki, Gifu, Japan), and Ms. K. Abe (Department of Molecular and Cellular Neurobiology, Gunma University Graduate School of Medicine) for technical assistance. This work was partly supported by a Grant-in-Aid for Scientific Research (No. 25122704) from the Japan Society for the Promotion of Science to Y. Ishizaki. A part of this study is the result of 'Integrated Research on Neuropsychiatric Disorders' carried out under the Strategic Research program for Brain Sciences (SRPBS) by the Ministry of Education, Culture, Sports, Science and Technology of Japan (MEXT) and Japan Agency for Medical Research and Development (AMED). The authors declare no conflicts of interest.

All experiments were conducted in compliance with the ARRIVE guidelines.

## Supporting information

Additional supporting information may be found in the online version of this article at the publisher's web-site:

**Figure S1.** Axons were preserved in the demyelinating lesions in the ET-1-injected IC.

**Figure S2.** Representative images of double staining for NG2 and ED-1.

**Figure S3.** MVECs increased immature OLs but not mature OLs.

## References

- Arai K. and Lo E. (2009) An oligovascular niche: cerebral endothelial cells promote the survival and proliferation of oligodendrocyte precursor cells. *J. Neurosci.* **29**, 4351–4355.
- Arbab A. S., Yocum G. T., Rad A. M., Khakoo A. Y., Fellowes V., Read E. J. and Frank J. A. (2005) Labeling of cells with ferumoxides-protamine sulfate complexes does not inhibit function or differentiation capacity of hematopoietic or mesenchymal stem cells. *NMR Biomed.* **18**, 553–559.
- Bamford J., Sandercock P., Dennis M., Burn J. and Warlow C. (1991) Classification and natural history of clinically identifiable subtypes of cerebral infarction. *Lancet* **337**, 1521–1526.
- Conijn M. M. A., Kloppenborg R. P., Algra A., Mali W. P. T. M., Kappelle L. J., Vincken K. L., van der Graaf Y. and Geerlings M. I. and Group, f. t. S. S (2011) Cerebral small vessel disease and risk of death, ischemic stroke, and cardiac complications in patients with atherosclerotic disease: the Second Manifestations of ARterial disease-Magnetic Resonance (SMART-MR) Study. *Stroke* **42**, 3105–3109.
- Dore-Duffy P., Katychev A., Wang X. and Van Buren E. (2006) CNS microvascular pericytes exhibit multipotential stem cell activity. *J. Cereb. Blood Flow Metab.* **26**, 613–624.
- Fitzgerald M., Bartlett C. A., Harvey A. R. and Dunlop S. A. (2010) Early events of secondary degeneration after partial optic nerve transection: an Immunohistochemical Study. *J. Neurotrauma* **27**, 439–452.
- Gadea A., Aguirre A., Haydar T. F. and Gallo V. (2009) Endothelin-1 regulates oligodendrocyte development. *J. Neurosci.* **29**, 10047–10062.
- Hacke W., Kaste M., Bluhmki E. *et al.* (2008) Thrombolysis with alteplase 3 to 4.5 hours after acute ischemic stroke. *N. Engl. J. Med.* **359**, 1317–1329.
- Hayashi T., Abe K. and Itoyama Y. (1998) Reduction of ischemic damage by application of vascular endothelial growth factor in rat brain after transient ischemia. *J. Cereb. Blood Flow Metab.* **18**, 887–895.
- Ishikawa H., Tajiri N., Shinozuka K. *et al.* (2013) Vasculogenesis in experimental stroke after human cerebral endothelial cell transplantation. *Stroke* **44**, 3473–3481.
- Ivanova A., Nakahira E., Oba A., Wada T., Takebayashi H., Spassky N., Levine J., Zalc B. and Ikenaka K. (2003) Evidence for a second wave of oligodendrogenesis in the postnatal cerebral cortex of the mouse. *J. Neurosci. Res.* **73**, 581–592.
- Jones L. L., Yamaguchi Y., Stallcup W. B. and Tuszynski M. H. (2002) NG2 is a major chondroitin sulfate proteoglycan produced after spinal cord injury and is expressed by macrophages and oligodendrocyte progenitors. *J. Neurosci.* **22**, 2792–2803.
- Khalilzada M., Dogan K., Ince C. and Stam J. (2011) Sublingual microvascular changes in patients with cerebral small vessel disease. *Stroke* **42**, 2071–2073.
- Lecrux C., McCabe C., Weir C. J., Gallagher L., Mullin J., Touzani O., Muir K. W., Lees K. R. and Macrae I. M. (2008) Effects of magnesium treatment in a model of internal capsule lesion in spontaneously hypertensive rats. *Stroke* **39**, 448–454.
- Louissaint A., Rao S., Leventhal C. and Goldman S. A. (2002) Coordinated interaction of neurogenesis and angiogenesis in the adult songbird brain. *Neuron* **34**, 945–960.
- Miron V. E., Kuhlmann T. and Antel J. P. (2011) Cells of the oligodendroglial lineage, myelination, and remyelination. *Biochim. Biophys. Acta* **1812**, 184–193.
- Muramatsu R., Takahashi C., Miyake S., Fujimura H., Mochizuki H. and Yamashita T. (2012) Angiogenesis induced by CNS inflammation promotes neuronal remodeling through vessel-derived prostacyclin. *Nat. Med.* **18**, 1658–1664.
- Nishiyama A., Komitova M., Suzuki R. and Zhu X. (2009) Polydendrocytes (NG2 cells): multifunctional cells with lineage plasticity. *Nat. Rev. Neurosci.* **10**, 9–22.
- Nitkunan A., Barrick T. R., Charlton R. A., Clark C. A. and Markus H. S. (2008) Multimodal MRI in cerebral small vessel disease: its relationship with cognition and sensitivity to change over time. *Stroke* **39**, 1999–2005.
- Payne S. C., Bartlett C. A., Savigni D. L., Harvey A. R., Dunlop S. A. and Fitzgerald M. (2013) Early proliferation does not prevent the loss of oligodendrocyte progenitor cells during the chronic phase of secondary degeneration in a CNS white matter tract. *PLoS ONE* **8**, e65710.
- Porambo M., Phillips A. W., Marx J. *et al.* (2015) Transplanted glial restricted precursor cells improve neurobehavioral and neuropathological outcomes in a mouse model of neonatal white matter injury despite limited cell survival. *Glia* **63**, 452–465.

- Puentes S., Kurachi M., Shibasaki K., Naruse M., Yoshimoto Y., Mikuni M., Imai H. and Ishizaki Y. (2012) Brain microvascular endothelial cell transplantation ameliorates ischemic white matter damage. *Brain Res.* **1469**, 43–53.
- Rhodes K. E., Raivich G. and Fawcett J. W. (2006) The injury response of oligodendrocyte precursor cells is induced by platelets, macrophages and inflammation-associated cytokines. *Neuroscience* **140**, 87–100.
- Sandercock P., Wardlaw J. M., Lindley R. I., the IST-3 collaborative group *et al.* (2012) The benefits and harms of intravenous thrombolysis with recombinant tissue plasminogen activator within 6 h of acute ischaemic stroke (the third international stroke trial [IST-3]): a randomised controlled trial. *Lancet* **379**, 2352–2363.
- Schmid A., Schmitz J., Mannheim J. G., Maier F. C., Fuchs K., Wehr H. F. and Pichler B. J. (2013) Feasibility of sequential PET/MRI using a state-of-the-art small animal PET and a 1 T benchtop MRI. *Mol. Imaging Biol.* **15**, 155–165.
- Schonberg D. L., Popovich P. G. and McTigue D. M. (2007) Oligodendrocyte generation is differentially influenced by toll-like receptor (TLR) 2 and TLR4-Mediated intraspinal macrophage activation. *J. Neuropathol. Exp. Neurol.* **66**, 1124–1135.
- Shibasaki K., Suzuki M., Mizuno A. and Tominaga M. (2007) Effects of body temperature on neural activity in the hippocampus: regulation of resting membrane potentials by transient receptor potential vanilloid 4. *J. Neurosci.* **27**, 1566–1575.
- Shin H. Y., Kim J. H., Phi J. F., Park C.-K., Kim J. E., Kim J.-H., Paek S. H., Wang K.-C. and Kim D. G. (2008) Endogenous neurogenesis and neovascularization in the neocortex of the rat after focal cerebral ischemia. *J. Neurosci. Res.* **86**, 356–367.
- Sun J., Sha B., Zhou W. and Yang Y. (2010) VEGF-mediated angiogenesis stimulates neural stem cell proliferation and differentiation in the premature brain. *Biochem. Biophys. Res. Commun.* **394**, 146–152.
- Szabó C. A., Deli M. A., Ngo T. K. and Joó F. (1997) Production of pure primary rat cerebral endothelial cell culture: a comparison of different methods. *Neurobiology (Budapest, Hungary)* **5**, 1–16.
- Uemura M., Kasahara Y., Nagatsuka K. and Taguchi A. (2012) Cell-based therapy to promote angiogenesis in the brain following ischemic damage. *Curr. Vasc. Pharmacol.* **10**, 285–288.
- Wardlaw J. M., Smith E. E., Biessels G. J. *et al.* (2013) Neuroimaging standards for research into small vessel disease and its contribution to ageing and neurodegeneration. *Lancet Neurol.* **12**, 822–838.
- Yuen T. J., Silbereis J. C., Griveau A., Chang S. M., Daneman R., Fancy S. P. J., Zahed H., Maltepe E. and Rowitch D. H. (2014) Oligodendrocyte-encoded HIF function couples postnatal myelination and white matter angiogenesis. *Cell* **158**, 383–396.
- Zhang Z. G., Zhang L., Jiang Q., Zhang R. L., Davies K., Powers C., van Bruggen N. and Chopp M. (2000) VEGF enhances angiogenesis and promotes blood-brain barrier leakage in the ischemic brain. *J. Clin. Invest.* **106**, 829–838.